Application of a statistical raindrop canting angle model on terrestrial and satellite links

J. Howard, B.Sc.(Eng.), D.U.C., M.Sc., Ph.D., C.Eng., M.I.E.E., Sen.Mem.I.E.E.

Indexing terms: *Radiowave propagation, Satellite links and space communication, Rain, Raindrop canting angle, Crosspolarisation, Turbulence*

Abstract: A statistical model estimating the mean and standard deviation of each drop-size canting angle, assuming Gaussian canting angle distributions, is presented. The model utilises the one-dimensional energy spectrum of horizontal turbulence given by F.B. Smith, and, using the differential equation for the horizontal drop movement, it calculates the mean and standard deviation of each drop-size canting angle. Comparison with M.J. Saunders's work shows good agreement. Application of the model to terrestrial and satellite links shows that, for rain alone, the crosspolarisation discrimination variations for satellite paths are much higher than in the terrestrial case, and that the crosspolarisation discrimination mean values are lower for terrestrial paths.

1 Introduction

Current interest in microwave propagation studies through precipitation particles has been prompted by proposals for terrestrial and satellite communication systems operating above 10 GHz. At these frequencies the presence of precipitation particles in the transmission medium causes attenuation and depolarisation of the transmitted radiation. Both effects may represent a severe limitation on system performance, and, in particular, the depolarisation effect is of considerable importance in the possibility of using two orthogonal polarisations as separate communication channels in future satellite and terrestrial communication systems.

Rain is one of the principal agents causing attenuation and depolarisation of the transmitted radiation in both terrestrial and satellite paths. In 1973, Watson and Arbabi [1] showed that the cause of rain-induced crosspolarisation was the canting of raindrops. In 1976, Brussaard [2] published his well known meteorological model for crosspolarisation due to rain, where he gave a physical explanation of raindrop canting. He showed that vertical wind gradients are a cause of canting, and he employed a model for the dependence of wind speed on height to calculate values of mean raindrop canting angles for heights up to 300 m. Howard and Mathews [3] published a paper extending Brussard's model to include estimates of mean raindrop canting angles on satellite paths. In addition to the mean horizontal wind changes with height, it is reasonable to assume that canting angle variations owing to wind fluctuations with time can cause crosspolarisation discrimination scintillations about a mean value. A suggestion that this is so was made by Semplak [4] in 1974. Since then, several workers [5–9] have published statistical models predicting crosspolarisation discrimination values, by assuming a mean path angle and a Gaussian distribution with a variance that provides a suitable spread for their crosspolarisation discrimination data. Maher and Murphy [10] calculated the variation of a raindrop canting angle as a function of wind velocity in a town environment*. They showed that the wind fluctuated in a sinusoidal manner with a frequency of 0.5 Hz. Howard and Gerogiokas [11] published a statistical raindrop canting angle model employing the one-dimensional energy spectrum of turbulence given by Davenport [12]. Later Howard [13] improved on the accuracy of the model by using the turbulence equations given by Smith [14]. Using the values for the mean and standard deviation of canting angle against raindrop size calculated by Howard and Gerogiokas [11], Moupfouma [15] published in a letter a theoretical model for calculating rain-induced crosspolarisation.

In this paper, the statistical model of Howard [13] is extended and applied to calculate variations of crosspolarisation discrimination values for terrestrial and satellite links. The statistical model presented here relates turbulence to the reaction of the raindrop canting angle to this turbulence. It is assumed that in general a wind spectrum exists, and that, within the turbulent boundary layer, the direction of the mean wind is constant [16] for the case of neutral or near neutral atmospheric conditions (i.e. purely mechanical turbulence), a case most appropriate in a precipitation environment [12]†. Using the differential equation describing the horizontal drop movement, a canting angle 'transfer function' is developed. Applying the horizontal wind velocity spectrum as 'input' and using Taylor's series [17], the 'response' of the drop (i.e. the mean and variance of its canting angle) is estimated. Application of the model to terrestrial and satellite links shows that large variations of the crosspolarisation discrimination values may exist, especially in satellite-to-earth paths.

2 Theory

Turbulence consists of quasirandom motions correlated in time and space, generated within the two lower km of the atmosphere as a result of the drag of the underlying surface on the wind, and by buoyancy forces when the lower layers are warmed by contact with the ground. Being essentially stochastic, turbulence has a basic random content consistent with some bounded probability distribution, while at the same time being correlated in both time and space.

The spectral components which compose a deterministic waveform are themselves deterministic. Thus the nth spectral component may be represented by

$$Un(t) = U(nf) \cos (2\pi nft + \alpha(nf)) \quad (1)$$

where all the variables have their usual meaning.

Paper 3641F (E9, E8, E11), first received 14th March and in revised form 10th October 1984

The author is with the Narda Microwave Corporation, 435 Moreland Road, Hauppauge, NY 11788, USA

* MURPHY, P.J.: personal communication

† Also SMITH, F.B.: personal communication

In the case of turbulence, the spectral components are themselves random processes. Thus, in eqn. 1, $U(nf)$ and $\alpha(nf)$ are random variables of amplitude and phase, and $Un(t)$ represents an ensemble of sample wind velocity functions, one sample function for each possible set of values of $U(nf)$ and $\alpha(nf)$. The sample functions are each deterministic waveforms; they are pure sinusoids differing from one another in phase and amplitude, depending on the value of $U(nf)$ and $\alpha(nf)$.

The differential equation for the horizontal drop movement is given by [2]

$$\frac{dV(t)}{dt} + \frac{g}{V_v} V(t) = \frac{g}{V_v} U(t) \tag{2}$$

where

$V(t)$ = horizontal drop velocity
V_v = vertical drop velocity, assumed to be constant and equal to the terminal velocity in stagnant air
$U(t)$ = wind velocity at the position of the drop
g = gravitational constant

Eqn. 2 is a linear differential equation of the first order, and its solution for the mean horizontal wind velocity (i.e. the DC component) is given in Reference 3 for the case of neutral or near neutral atmospheric conditions, using a logarithmic wind profile. For completeness, it is repeated here in the Appendix.

Applying now eqn. 1 in eqn. 2, we have

$$V_n(t) = V(nf) \cos (2\pi nft + \beta(nf)) \tag{3}$$

In this case, $V(nf)$ and $\beta(nf)$ are random variables of amplitude and phase, and $Vn(t)$ represents an ensemble of sample raindrop velocity functions. Eqns. 1 and 3 may be rewritten as

$$Un(t) = \frac{U(nf)}{2} (e^{j(2\pi nft + \alpha(nf))} + e^{-j(2\pi nft + \alpha(nf))}) \tag{4}$$

and

$$Vn(t) = \frac{V(nf)}{2} (e^{j(2\pi nft + \beta(nf))} + e^{-j(2\pi nft + \beta(nf))}) \tag{5}$$

Generalising eqns. 4 and 5 for any frequency f and introducing $\omega = 2\pi f$, we obtain, using eqns. 2, 4 and 5, the following equations:

$$\frac{V(f)}{2}\left(\frac{g}{V_v} + j\omega\right) e^{j(\omega t + \varphi(f))} = \frac{U(f)}{2} \frac{g}{V_v} e^{j\omega t} \tag{6a}$$

$$\frac{V(f)}{2}\left(\frac{g}{V_v} - j\omega\right) e^{-j(\omega t + \varphi(f))} = \frac{U(f)}{2} \frac{g}{V_v} e^{-j\omega t} \tag{6b}$$

$$V(f) \cos (\omega t + \varphi(f)) = \frac{U(f)}{2}\left(\frac{g/V_v}{g/V_v + j\omega} e^{j\omega t} + \frac{g/V_v}{g/V_v - j\omega} e^{-j\omega t}\right) \tag{7}$$

where

$$\varphi(f) = \beta(f) - \alpha(f)$$

The canting angle θ of a raindrop due to wind variations is given by [2]

$$\tan \theta = \frac{U - V}{V_v} \tag{8}$$

Eqn. 8 may now be written as

$$\begin{aligned}
\tan \theta &= \frac{U(f) \cos \omega t - V(f) \cos (\omega t + \varphi(f)}{V_v} \\
&= \frac{U(f)}{2V_v}\left[\left(1 - \frac{g/V_v}{g/V_v + j\omega}\right) e^{j\omega t} + \left(1 - \frac{g/V_v}{g/V_v - j\omega}\right) e^{-j\omega t}\right] \\
&= \frac{U(f)}{V_v} \frac{1}{\sqrt{1 + (g/\omega V_v)^2}} \times \left[\frac{e^{j(\omega t + \tan^{-1} g/\omega V_v)} + e^{-j(\omega t + \tan^{-1} g/\omega V_v)}}{2}\right] \\
&= \frac{U(f)}{V_v} \frac{1}{\sqrt{1 + (g/\omega V_v)^2}} \cos (\omega t + \tan^{-1} g/\omega V_v)
\end{aligned} \tag{9}$$

The variable $1/(V_v(1 + (g/\omega V_v)^2)^{1/2})$ is the amplitude of a 'transfer function' relating $\tan \theta$ to a sinusoidal wind variation. $\tan^{-1} (g/\omega V_v)$ is the phase delay introduced by the transfer function. The energy spectrum of $\tan \theta$, i.e. of the output, can be obtained by applying this transfer function to the horizontal wind velocity energy spectrum $S(f)$. Integrating this output spectrum over all frequencies, the variance of $\tan \theta$ can be calculated. Thus

$$\begin{aligned}
\sigma^2_{\tan \theta} &= \int_0^\infty |TF|^2 S(f)\, df \\
&= \int_0^\infty \frac{1}{V_v^2(1 + (g/\omega V_v)^2)} S(f)\, df
\end{aligned} \tag{10}$$

The one-dimensional energy spectrum $S(f)$ of turbulence can be expressed [14] as

$$S(f) = 0.15 U^{2/3} \varepsilon^{2/3} f^{-5/3} \tag{11}$$

in m/s^3, and where

f = frequency of wind variation
ε = rate of turbulence energy dissipation
U = mean horizontal wind velocity at the height of interest

In neutral or near neutral atmospheric conditions, the rate of dissipation ε is given by

$$\varepsilon = U_*^2 \frac{dU}{dh} \tag{12}$$

where

U_* = friction velocity (see Appendix)
h = height of interest

In the case of unstable atmospheric conditions, the rate of turbulent energy ε is virtually independent of the height h and the wind velocity U. Thus, in convective turbulence, ε being virtually a constant, the energy spectrum is given by [14]

$$S(f) = 0.14 U^{2/3} f^{-5/3} \tag{13}$$

In the case where there is precipitation, the atmosphere is most likely to be neutral or near neutral. This is the case, as† (i) cloud cover will reduce incoming solar radiation so that turbulence will be losing energy, but (ii) the ground will be wet, and hence most of the available energy will go into evaporation, thus adding to the turbulent energy.

† SMITH, F.B.: personal communication

The combination of the above two conditions will produce energy equilibrium in the turbulence, and hence the atmospheric conditions will be neutral or near neutral. In addition, although the turbulence in the atmosphere is both convective and mechanical in origin, in high winds, even without any precipitation present, convective turbulence plays a relatively minor role [12]. The reason for this is that whereas mechanical turbulence rapidly increases with wind velocity, convective turbulence, if anything, tends to be 'damped out' by the powerful mixing action caused by the mechanical turbulence; the latter prevents the necessary thermal instabilities from arising, and tends to reduce the atmosphere to a state of neutral stability.

In addition to the variance of tan θ given by eqn. 10, the mean value of tan θ is given by eqn. 39 (see Appendix). Assuming that the probability density function $f(\theta)$ of θ is 'smooth' [17] about the mean value η of tan θ, the mean and variance of the canting angle θ can be estimated using the mean and variance of tan θ, and by employing the Taylor series expansion. In the case where $f(\theta)$ is a Gaussian distribution, this is readily seen to be true. Thus, in general, if the mean value η and the variance σ_x^2 of the random variable x are known, the random variable $g(x)$ has the following estimates of mean and variance:

$$E(g(x)) \approx g(\eta) + g''(\eta)\frac{\sigma_x^2}{2} \tag{14}$$

and

$$\sigma_{g(x)}^2 \approx g^2(\eta) + [(g'(\eta))^2 + g(\eta)g''(\eta)]\sigma_x^2 - \left(g(\eta) + g''(\eta)\frac{\sigma_x^2}{2}\right)^2 \tag{15}$$

respectively. Using

$x = \tan\theta$
$\eta = \tan\theta_0$
$\sigma_x^2 = \sigma_{\tan\theta}^2$
$g(x) = \tan^{-1}(\tan\theta)$

we obtain, employing eqns. 14 and 15, the following estimates for the mean and variance values of the canting angle θ:

$$E(\theta) \approx \tan^{-1}(\tan\theta_0) - \tan\theta_0 \cos^4\theta_0 \sigma_{\tan\theta}^2 \tag{16}$$

$$\sigma_\theta^2 \approx \cos^4\theta_0 \sigma_{\tan\theta}^2 + \tan^2\theta_0 \cos^8\theta_0 \sigma_{\tan\theta}^4 \tag{17}$$

Eqns. 16 and 17 can now be used to estimate crosspolarisation discrimination variations in the presence of rain.

The propagation of microwaves in the presence of precipitation may be described by

$$\begin{pmatrix} E_h \\ E_v \end{pmatrix}_{z=z_1} = \begin{pmatrix} T_{11} & T_{12} \\ T_{21} & T_{22} \end{pmatrix} \begin{pmatrix} E_h \\ E_v \end{pmatrix}_{z=0} \tag{18}$$

where the subscripts h, v denote horizontal and vertical polarisations, respectively, and $z(=0 \rightarrow z_1)$ is a thick layer of precipitation.

The elements of the transmission matrix $[T_{ij}]$ are given by

$$\left.\begin{aligned} T_{11} &= \frac{1}{(\gamma_v - \gamma_h)}((\gamma_v - qG_{hh})\,e^{-\gamma_h z} - (\gamma_h - qG_{hh})\,e^{-\gamma_v z}) \\ T_{22} &= \frac{1}{(\gamma_v - \gamma_h)}(-(\gamma_h - qG_{hh})\,e^{-\gamma_h z} + (\gamma_v - qG_{hh})\,e^{-\gamma_v z}) \\ T_{12} = T_{21} &= \frac{1}{(\gamma_v - \gamma_h)}qG_{hv}(e^{-\gamma_h z} - e^{-\gamma_v z}) \end{aligned}\right\} \tag{19}$$

with

$$\left.\begin{aligned} G_{hh} &= \int_R (S_{II}(0)\cos^2\theta + S_I(0)\sin^2\theta)N(R)\,dR \\ G_{vv} &= \int_R (S_{II}(0)\sin^2\theta + S_I(0)\cos^2\theta)N(R)\,dR \\ G_{hv} &= \int_R (S_{II}(0) - S_I(0))\frac{\sin 2\theta}{2}N(R)\,dR \end{aligned}\right\} \tag{20}$$

and

$$\left.\begin{aligned} \gamma_v &= q\left(\frac{G_{hh}+G_{vv}}{2}\right) - q\left(\frac{G_{hh}-G_{vv}}{2}\right)\sqrt{1+\frac{4G_{hv}^2}{(G_{hh}-G_{vv})^2}} \\ \gamma_h &= q\left(\frac{G_{hh}+G_{vv}}{2}\right) + q\left(\frac{G_{hh}-G_{vv}}{2}\right)\sqrt{1+\frac{4G_{hv}^2}{(G_{hh}-G_{vv})^2}} \end{aligned}\right\} \tag{21}$$

where $S_I(0)$ and $S_{II}(0)$ are the forward scattering complex scalar amplitudes for vertical and horizontal polarisations, respectively, $N(R)$ is the number of drops/m^3 for each drop size, where R denotes the radius, $q = 2\pi/K^2$ with $K = 2\pi/d$, d being the wavelength of the microwave signal.

Crosspolarisation discrimination is defined as the ratio of the copolar signal amplitude to the crosspolar signal amplitude in dB when one polarisation is transmitted and the copolar and crosspolar signals are received separately. Thus, using the notation of eqn. 18, we obtain for vertical and horizontal polarisations the expressions

$$XPD_V = 20\log_{10}\left|\frac{T_{22}}{T_{12}}\right| \tag{22}$$

and

$$XPD_H = 20\log_{10}\left|\frac{T_{11}}{T_{21}}\right| \tag{23}$$

3 Computations

3.1 Comparison with Saunders's [18] results

Before applying the statistical raindrop canting angle model to estimate the crosspolarisation discrimination values for terrestrial and satellite paths, a check was made against the distribution of canting angles during two rainstorms given in a paper by Saunders [18], using the images of 463 raindrops obtained with a raindrop camera by personnel at the Illinois State Water Survey [19, 20]†. To compare Saunders's results with the model presented here, further information is needed in addition to the mean horizontal wind speed of 15 m/s and the precipitation rate of 28 mm/h provided, namely:

(*a*) the height of the raindrop camera

(*b*) the type of terrain where the measurements were taken

(*c*) the height of the anemometer.

The information supplied to the author †‡ indicated that:

(*d*) the height of the camera was approximately 1.5 m

(*e*) the type of terrain was 'flat countryside with some form of vegetation'

(*f*) the height of the anemometer was assumed to be approximately 10 m.

For the type of terrain indicated above the mean friction velocity U_* was calculated to be 1.3 m/s, using a terrain constant $z_0 = 0.1$ m in eqn. 34 (see Appendix). With

† JONES, D.M.A.: personal communication
‡ SAUNDERS, M.J.: personal communication

the help of eqns. 10, 16, 17 and 39 (see Appendix), the mean and standard deviation of the canting angle of each raindrop size were calculated. The results are tabulated in Table 1, with Table 2 presenting results for a mean horizontal wind velocity of 10 m/s. In the latter case, the mean friction velocity U_* was calculated to be 0.87 m/s.

Table 1: Mean and standard deviation of canting angle

Drop radius, m	$E(\theta)$, deg	σ_θ, deg
0.00025	8.17	44.91
0.00050	21.57	25.76
0.00075	25.07	20.47
0.00100	26.45	17.89
0.00125	27.07	16.32
0.00150	27.32	15.42
0.00175	27.42	14.87
0.00200	27.46	14.54
0.00225	27.48	14.37
0.00250	27.48	14.28
0.00275	27.48	14.24
0.00300	27.48	14.23
0.00325	27.48	14.23

Mean horizontal wind velocity $U = 15$ m/s, measured at height $h = 10$ m; height of observations $h = 1.5$ m, friction velocity $U_* = 1.303$ m/s

Table 2: Mean and standard deviation of canting angle

Drop radius, m	$E(\theta)$, deg	σ_θ, deg
0.00025	10.66	27.17
0.00050	17.30	16.64
0.00075	19.09	13.51
0.00100	19.75	11.90
0.00125	20.00	10.89
0.00150	20.06	10.30
0.00175	20.07	9.93
0.00200	20.05	9.71
0.00225	20.04	9.59
0.00250	20.03	9.53
0.00275	20.03	9.50
0.00300	20.03	9.50
0.00325	20.03	9.50

Mean horizontal wind velocity $U = 10$ m/s, measured at height $h = 10$ m; height of observations $h = 1.5$ m, friction velocity $U_* = 0.87$ m/s

A Gaussian canting angle distribution was assumed for each drop size, with each drop-size distribution being weighted according to the number of drops for each size [21] (see Table 3). In Fig. 1, the fraction of raindrop population with canting angles $\geq\theta°$ and $\leq -\theta°$ (as in Saunders's Fig. [18]) is plotted together with Saunders's graph for the 28 mm/h precipitation rate and 15 m/s mean horizontal wind velocity. From Fig. 1 (or Table 1), a mean effective canting angle of 14.1° is obtained with a standard deviation of 38.6°.

Table 3: Weighting applied on individual Gaussian drop-size canting angle distribution

R, cm	Weighting
0.025	0.646
0.050	0.185
0.075	0.099
0.100	0.045
0.125	0.017
0.150	0.006
0.175	0.002
0.200	0.001
0.225	0.000
0.250	0.000
0.275	0.000
0.300	0.000
0.325	0.000

Precipitation rate = 25 mm/h

3.2 Application of model to a terrestrial link

The terrestrial link considered had a path length of 3 km, and the transmitting and receiving antennas were assumed to be at a height of 10 m. With a signal frequency of 11 Ghz, two mean horizontal velocities were considered, 10 m/s and 15 m/s, and four precipitation rates, 25 mm/h, 50 mm/h, 100 mm/h and 150 mm/h, were used. The mean friction velocities U_* mentioned above were assumed, their values associated with a terrain of large open fields (200–500 m). The path length was separated into 50 m long layers.

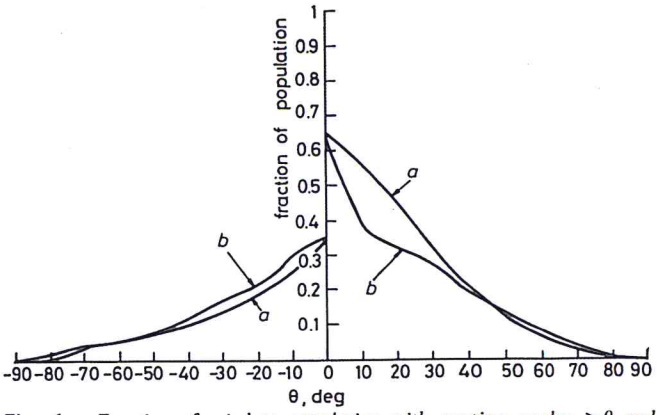

Fig. 1 *Fraction of raindrop population with canting angles $\geq\theta$ and $\leq -\theta$*

Shown as curves *a*. Horizontal wind velocity $U = 15$ m/s, height $h = 1.5$ m, precipitation rate 25 mm/h. Comparison with Saunders's results (curves *b*) for 28 mm/h precipitation rate

The horizontal wind velocities at any two points within each layer were taken as equal, with wind velocities between layers considered completely uncorrelated. The necessary length of the layers was calculated using

$$R(x) = \frac{1}{\sigma^2}\int_0^\infty S(f)\cos\frac{2\pi fx}{U}\,df \tag{24}$$

where $R(x)$ is the spatial correlation function of velocity and σ^2 is the wind velocity variance, given by

$$\sigma^2 = \int_0^\infty S(f)\,df \tag{25}$$

For a layer length of 50 m, the correlation function $R(x)$ is very nearly equal to 0.5. Therefore, if two points in space were separated by a distance greater than 50 m, then the wind velocities at these points were assumed to have a correlation function $R(x)$ equal to zero. Conversely, if the distance between two points in space was less than 50 m, the wind velocities at the points were assumed to have a correlation function $R(x)$ equal to unity. In addition to the above, the precipitation rate was assumed to be constant along the whole of the path.

Using the system of layers described above, eqn. 18 becomes

$$\begin{pmatrix} E_h \\ E_v \end{pmatrix}_{z=z_1} = \begin{pmatrix} T_{11} & T_{12} \\ T_{21} & T_{22} \end{pmatrix}_{l_n} \begin{pmatrix} T_{11} & T_{12} \\ T_{21} & T_{22} \end{pmatrix}_{l_{n-1}} \begin{pmatrix} T_{11} & T_{12} \\ T_{21} & T_{22} \end{pmatrix}_{l_1} \times \begin{pmatrix} E_h \\ E_v \end{pmatrix}_{z=0} \tag{26}$$

As drops fall with vertical velocities that increase with their size, their 'past history' will also depend on drop size. For a terrestrial link, the different sized drops will arrive at the observation height having canting angles that are uncorrelated.

Attenuation and crosspolarisation discrimination calculations for vertical and horizontal polarisations were made

by repeated application of eqn. 26. Eqns. 16 and 17 provided estimates for the mean and variance of each drop size. Assuming a Gaussian distribution for each drop size, random canting angles were generated. Thus, all drops in each size were tilted at the same angle. This is perfectly valid, as drops of the same size having the same 'transfer function' will respond with the same canting angle to any wind velocity input.

Some of the results of the above computations are shown in Figs. 2 and 3. Fig. 2 shows a plot of cross-

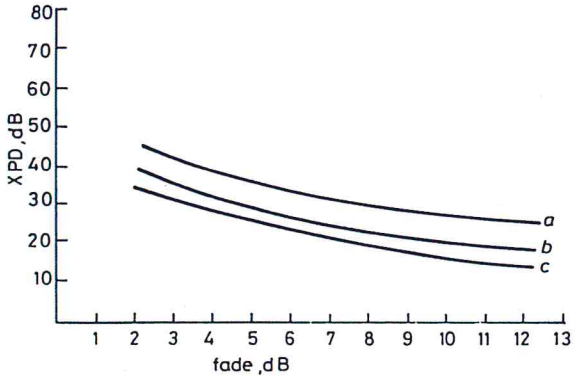

Fig. 2 *Crosspolarisation discrimination against fade for terrestrial link*

Frequency $f = 11$ GHz, horizontal wind velocity $U = 15$ m/s, friction velocity $U_* = 1.3$ m/s at a height $h = 10$ m, total path length $l = 3$ km. Curves a and c are the maximum and minimum crosspolarisation discrimination bounds, respectively, and curve b is the mean value of the crosspolarisation discrimination

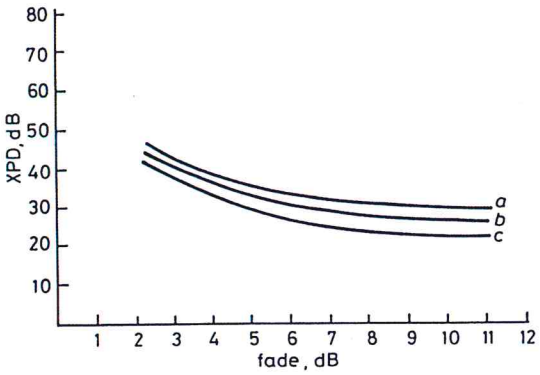

Fig. 3 *Crosspolarisation discrimination against fade for terrestrial link*

Frequency $f = 11$ GHz, horizontal wind velocity $U = 10$ m/s, friction velocity $U_* = 0.87$ m/s at a height $h = 10$ m, total path length $l = 3$ km. Curves a and c are the maximum and minimum crosspolarisation discrimination bounds, respectively, and curve b is the mean value of the crosspolarisation discrimination

polarisation discrimination values for vertical polarisation against fade for a mean horizontal velocity of $U = 15$ m/s. The three curves represent the mean value and the minimum and maximum crosspolarisation discrimination bounds. The results for a mean horizontal wind velocity of $U = 10$ m/s are presented in Fig. 3.

3.3 Application of model to a satellite link

The elevation angle of the satellite path was taken to be 20° and precipitation was assumed to have been initiated at a height slightly higher than 1 km, so that the total precipitation medium length was 3 km. The precipitation rates, wind velocities and friction velocities were assumed to be the same as for the terrestrial case. The path length was separated into layers 50 m long. Although for the satellite link it may be argued that the layers should be changing with height, as the wind velocity increases with height (see eqn. 34), it can be shown that the spatial correlation function varies slowly with wind velocity, and therefore with height. What is more important is that the drop-size canting angles may not be considered uncorrelated. Thus, at the highest (i.e. 'starting') layer, all drops are subjected to the same wind velocity variations, and their response to wind velocity fluctuations is fully correlated. As the height decreases, owing to the fact that each drop size falls with different vertical velocity V_v, especially near the ground, then the past history of each drop size must be taken into account in order to correctly compute the crosspolarisation discrimination values. Thus drop sizes that had separated from the initial drop group by more than a certain height d were considered to be uncorrelated with the rest of that group. For the uncorrelated drops, each drop-size canting angle was computed independently. For drops that were correlated, once a drop-size canting angle was generated, the canting angle of each other drop size was fixed with the help of eqn. 39. The distance d changed with height, so as to keep the variation of the mean horizontal wind velocity for each d value the same. This variation was not more than 1%.

With this in mind, estimates of attenuation and crosspolarisation discrimination values were computed using eqns. 16, 17 and 26. Some of the results are presented in Figs. 4 and 5. Fig. 4 shows a plot of crosspolarisation dis-

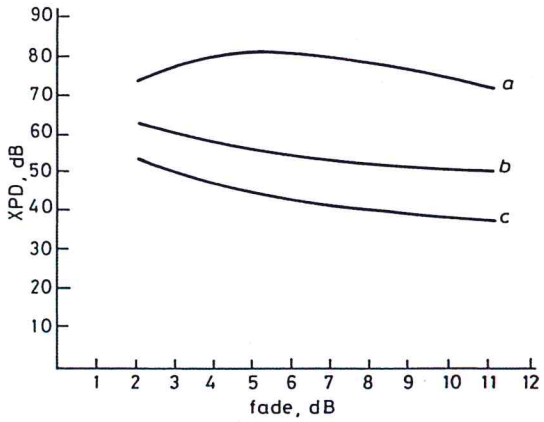

Fig. 4 *Crosspolarisation discrimination against fade for satellite link*

Frequency $f = 11$ GHz, horizontal wind velocity $U = 15$ m/s, friction velocity $U_* = 1.3$ m/s at a height $h = 10$ m, total path length $l = 3$ km. Curves a and c are the maximum and minimum crosspolarisation discrimination bounds, respectively, and curve b is the mean value of the crosspolarisation discrimination

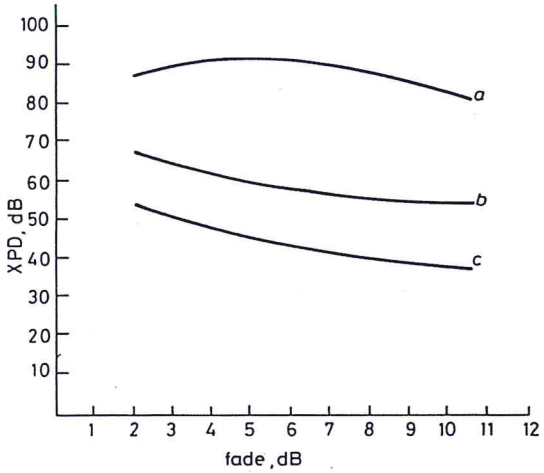

Fig. 5 *Crosspolarisation discrimination against fade for satellite link*

Frequency $f = 11$ GHz, horizontal wind velocity $U = 10$ m/s, friction velocity $U_* = 0.87$ m/s at a height $h = 10$ m, total path length $l = 3$ km. Curves a and c are the maximum and minimum crosspolarisation discrimination bounds, respectively, and curve b is the mean value of the crosspolarisation discrimination

crimination values for vertical polarisation against fade for a mean horizontal wind velocity of $U = 15$ m/s. As in the terrestrial case, the three curves represent the mean value and the minimum and maximum crosspolarisation discrimination bounds. The results for a mean horizontal

wind velocity of $U = 10$ m/s are shown in Fig. 5. Attenuation variations are small with wind fluctuations, and they were neglected in both the satellite and terrestrial cases.

Figs. 4 and 5 show much higher crosspolarisation discrimination variations than Figs. 2 and 3 (for the terrestrial case). In addition, the mean crosspolarisation discrimination levels for rain only are higher for satellite paths (see also Reference 3). To explain these results, the following are noted:

(*a*) The mean canting angle for each drop size is very nearly zero for heights above 500 m. As a result, the mean crosspolarisation discrimination increases, as the crosspolar amplitudes T_{12} and T_{21} in eqns. 22 and 23 have their values diminished

(*b*) Although for large heights the individual drop-size canting angle standard deviations also decrease, any variations of the drop canting angles greatly influence the small-valued crosspolar signal amplitudes, especially as most of the drops are now correlated, and respond in a similar fashion to any wind variations. The result is that crosspolarisation discrimination variations now become much higher.

4 Conclusions and discussion

In this paper a statistical model for estimating the mean and standard deviation of each drop-size canting angle has been presented. Computations of crosspolarisation discrimination values for terrestrial and satellite links using the model have been given.

The mathematical analysis presented is simplified in that only the one-dimensional spectral expansion of turbulence has been used. In addition, although for the strong winds considered no change of wind direction is expected to occur, for lighter winds, direction as well as wind speed may vary with time. Similarly, raindrop oscillations and drop-shape variations [22] may be of importance at heights above the surface layer, especially in convective-type turbulence.

For a more comprehensive and complete theoretical precipitation model, it is evident that further investigation is required. Clearly, there is much to be done.

5 References

1 WATSON, P.A., and ARBABI, M.: 'Rainfall crosspolarisation at microwave frequencies', *Proc. IEE*, 1973, **120**, (4), pp. 413–418
2 BRUSSAARD, G.: 'A meteorological model for rain-induced cross-polarisation', *IEEE Trans.*, 1976, **AP-24**, pp. 5–11
3 HOWARD, J., and MATHEWS, N.A.: 'Crosspolarisation of microwaves due to rain on a satellite to earth path', *ibid.*, 1979, **AP-27**, pp. 890–891
4 SEMPLAK, R.A.: 'Measurements of rain-induced polarisation rotation at 30.9 GHz', *Radio Sci.*, 1974, **9**, pp. 425–429
5 UZUNOGLU, N.K., EVANS, B.G., and HOLT, A.R.: 'Scattering of electromagnetic radiation by precipitation particles and propagation characteristics of terrestrial and space communication systems', *Proc. IEE*, 1977, **124**, (5), pp. 417–424
6 NOWLAND, W.L., OLSEN, R.L., and SHKAROFSKY, I.P.: 'Theoretical relationship between rain depolarisation and attenuation', *Electron. Lett.*, 1977, **13**, pp. 676–678
7 DILWORTH, I.J., and EVANS, B.G.: 'Cumulative crosspolarisation and canting angle distribution', *ibid.*, 1979, **15**, pp. 603–604
8 KANELLOPOULOS, J.D.: 'Statistical predictions during rain for dual-polarisation systems'. Proceedings of 9th European microwave conference, Brighton, England, September 1979, pp. 677–681
9 KANELLOPOULOS, J.D., and CLARKE, R.H.: 'A method for calculating rain depolarisation distributions on microwave paths', *Radio Sci.*, 1981, **16**, pp. 55–65
10 MAHER, B.O., and MURPHY, P.J.: 'Variation of canting-angle distribution as a function of wind velocity', *Electron. Lett.*, 1977, **13**, pp. 567–568
11 HOWARD, J., and GEROGIOKAS, M.: 'A statistical raindrop canting model', *IEEE Trans.*, 1982, **AP-30**, pp. 141–147
12 DAVENPORT, A.G.: 'The spectrum of horizontal gustiness near the ground in high winds', *Q. J. R. Meteorol. Soc.*, 1961, **87**, pp. 194–211
13 HOWARD, J.: 'A statistical canting angle model using horizontal wind energy spectra'. IEEE MELECON, Athens, Greece, May 1983
14 SMITH, F.B.: 'Turbulence in the atmospheric boundary layer', *Sci. Prog.*, 1975, **62**, pp. 127–151
15 MOUPFOUMA, F.: 'Theoretical model for calculating rain-induced crosspolarisation', *Electron. Lett.*, 1983, **19**, pp. 467–469
16 KERR, D.E. (Ed.): 'Propagation of short radio waves' (Dover Publications, New York, 1951)
17 PAPOULIS, A.: 'Probability, random variables and stochastic processes' (McGraw-Hill, Tokyo, 1965)
18 SAUNDERS, M.J.: 'Crosspolarisation at 18 and 30 GHz due to rain', *IEEE Trans.*, 1971, **AP-19**, pp. 273–277
19 JONES, D.M.A., and DEAN, L.A.: 'A raindrop camera'. US Army Signal Corps Engineering Laboratories, Fort Monmouth, New Jersey Research Report 3, Contract DA-36-039 SC-42446, December 1953
20 JONES, D.M.A.: 'The shape of raindrops', *J. Meteorol.*, 1959, **16**, pp. 504–510
21 LAWS, J.W., and PARSONS, D.A.: 'The relation of raindrop size intensity', *EOS Trans. Am. Geophs. Union*, 1943, **24**, pp. 432–460
22 BEARD, K.V., and JAMESON, A.R.: 'Raindrop canting', *J. Atmos. Sci.*, 1983, **40**, pp. 448–454
23 ABRAMOWITZ, M., and STEGUN, I.A.: 'Handbook of mathematical functions' (Dover Publications, New York, 1972)

6 Appendix: Calculation of the mean canting angle θ_0

The differential equation for the horizontal drop movement is given by

$$\frac{dV(t)}{dt} + \frac{g}{V_v} V(t) - \frac{g}{V_v} U(t) = 0 \tag{27}$$

where V, U, V_v and g are defined above.

We note that eqn. 27 is a linear differential equation of the first order, and so has the following general solution:

$$V(t) = C\, e^{-(g/V_v)t} + \frac{g}{V_v} e^{-(g/V_v)t} \int_0^t U(\tau)\, e^{(g/V_v)\tau}\, d\tau \tag{28}$$

Assuming that there is no updraught, the height of the drop follows from

$$h(t) = h(0) - V_v t \tag{29}$$

Using eqn. 29 in eqn. 27, we have

$$\frac{dV(h)}{dh} - \frac{g}{V_v^2} V(h) + \frac{g}{V_v^2} U(h) = 0 \tag{30}$$

The solution of eqn. 30 is given by

$$V(h) = C_1\, e^{(g/V_v^2)h} - \frac{g}{V_v^2} e^{(g/v_v^2)h} \int_0^h e^{-(g/V_v^2)y} \times U(y)\, dy \tag{31}$$

where

$$C_1 = \lim_{h\to\infty}\left[V(h)\, e^{-(g/V_v^2)h} + \frac{g}{V_v^2}\int_0^h e^{-(g/V_v^2)y} U(y)\, dy \right]$$

$$= 0 + \frac{g}{V_v^2}\int_0^\infty e^{-(g/V_v^2)y} U(y)\, dy \tag{32}$$

Using eqn. 32 in eqn. 31, we obtain

$$V(h) = \frac{g}{V_v^2} e^{(g/V_v^2)h}\left[\int_0^\infty e^{-(g/V_v^2)y} U(y)\, dy - \int_0^h e^{-(g/V_v^2)y} U(y)\, dy\right] = \frac{g}{V_v^2} e^{(g/V_v^2)h} \times \int_h^\infty e^{-(g/V_v^2)y} U(y)\, dy \tag{33}$$

For neutral conditions, the mean horizontal wind velocity varies with height in a logarithmic manner [14], as

$$U(y) = \frac{U_*}{K} \ln\left(\frac{y}{z_0}\right) \tag{34}$$

where U_* is the friction velocity, K is Von Karman's constant and z_0 is a constant depending on the terrain.

Therefore

$$V(h) = U(h) + \frac{U_*}{K} e^{(g/V_v^2)h} \int_h^\infty \frac{e^{-(g/V_v^2)y}}{y} dy \tag{35}$$

or

$$V(h) = U(h) + \frac{U_*}{K} e^{(g/V_v^2)h} \times \int_{(g/V_v^2)h}^\infty \frac{e^{-(g/V_v^2)y}}{(g/V_v^2)y} d(g/V_v^2)y \tag{36}$$

However, we note that [23]

$$\int_z^\infty \frac{e^{-t}}{t} dt = E_1(z) \tag{37}$$

where $E_1(z)$ is called the 'exponential integral'.

Using eqn. 37 in eqn. 36, we obtain

$$V(h) = U(h) + \frac{U_*}{K} e^{(g/V_v^2)h} E_1(g/V_v^2 h) \tag{38}$$

The mean canting angle for each raindrop can be obtained from

$$\tan \theta_0 = \frac{U(h) - V(h)}{V_v} = \frac{U_*}{KV_v} e^{(g/V_v^2)h} E_1(g/V_v^2 h) \tag{39}$$